



# IMPLEMENTATION OF GRID-CONNECTED PV INTEGRATED WITH HYBRID ENERGY STORAGE SYSTEM BY A POWER MANAGEMENT SCHEME

A V V Vishnu<sup>1</sup>, M.Murali<sup>2</sup>, Dr. A Hema Sekhar<sup>3</sup>, P.I.D.T.Baladuraikannan<sup>4</sup>

<sup>1</sup> PG Student, Electrical and Electronics Engineering, VEMU Institute of Technology

<sup>3</sup> Professor and HOD, Electrical and Electronics Engineering, VEMU Institute of Technology

<sup>2,4</sup> Associate Professor, Electrical and Electronics Engineering, VEMU Institute of Technology

**Abstract :** Integrating RESs into the distribution system threatens the reliability and security of the existing power grid. The reliability and consistency of the electricity provided by the system are significantly impacted by the unpredictability of renewable energy sources and fluctuations in demand. Microgrid power and energy storage devices are quite space intensive. Using grid connectivity and energy storage technologies like hybrid batteries and supercapacitors, this initiative aims to provide a solid foundation for solar energy management. The integration of a supercapacitor and a battery storage system allows for the rapid handling of both short-term and long-term power fluctuations, resulting in a more stable system and an easier time navigating fluctuations in PV output. How the grid and the battery are typically divided up in terms of average power is revealed by the battery's state of charge (SOC). Also provided is a method for controlling energy that is both practical and beneficial. Another benefit of using a supercapacitor is that it reduces stress on the battery system in the event of a sudden disparity between produced and required power. Simulations validate the efficacy and viability of the proposed energy management strategy.

**Index Terms –** Hybrid micro grid, power management, hybrid energy storage arrangement, super capacitor, battery

## I. INTRODUCTION

Energy savings are critical and natural energy sources are expanding swiftly, thus the power system uses green technology increasingly. The majority of photovoltaic (PV) systems use wind and sun power. Photovoltaic (PV) technology is the best and longest-lasting solution because to its low cost, great effectiveness, low maintenance, and reliability. Humidity, temperature, irradiance, and partial shadow can compromise a networked system's security [1]. Energy storage systems (ESSs) may increase microgrid dependability and safety, balance intermittent power sources like photovoltaics, and close the production-consumption power gap. Batteries are simple and have been the favoured energy storage method. Due to their high energy and low power density, batteries charge and discharge slowly. Because they charge and discharge faster than batteries, supercapacitors have higher power density and lower energy density. HESSs combine battery and supercapacitor features. Supercapacitors get short-term power from the HESS to enhance battery life [2]. Well-planned power tracking is needed for hybrid microgrids.

The proposed method assumes: maintaining a steady flow of electricity at a reasonable price; regulating the system's voltage and frequency; controlling the DC-link voltage; improving power characteristics; transitioning to a continuous and smooth operating mode; and maintaining energy storage devices' charge. The person said "[3]." Many hybrid microgrid electricity management systems have been researched. See also: An integrated power and control system is presented [4]. In order to govern the flow of electricity from generators to customers and back to the utility grid in an efficient and seamless manner, this technique employs a fixed control system. You may use the CAPMS with a PV battery system or the grid. We disregard worries about electricity quality. A single optimisation issue is generated by the system's efficient regulation of voltage and power. During emergencies, renewable energy sources and battery storage can be powered by a diesel engine. To guarantee energy supply, diesel engine issues including low fuel, slow starting, and frequent shutoffs must be resolved. In a DC microgrid that incorporates hybrid energy storage, a PI controller system may regulate the voltage on the DC bus and the distribution of power on an as-needed basis [6].

## II. SYSTEM ARCHITECTURE AND POWER MANAGEMENT SCHEME

A photovoltaic (PV) system with a hybrid energy storage system (HESS) and grid connection may be shown in Figure 2.1. The inductor (L1) and capacitors (C1, C2) are the namesakes of the quadratic boost converter. The user's input field is blank. If you would like

a piece of writing rewritten utilising advanced terminology that is both clear and exact, please send it my way.  $D_1$ ,  $D_2$ , and  $D_3$  are the diodes used in the quadratic boost converter. The voltages  $V_g$ ,  $V_{dc}$ , and  $V_B$  stand for the grid voltage, DC bus voltage, and battery voltage, respectively. The capacitors in the battery are marked as  $C_b$ , whereas those in the bidirectional converter are marked as  $C_{db}$ . A supercapacitor's capacitance value is called the " $C_{sc}$ " value. We can see the filter's capacitance,  $L_f$ , its resistance,  $R_f$ , and inductance,  $C_f$ , in the graph. The symbol  $V_{sc}$  is commonly used to represent the voltage at the supercapacitor's terminals. When no load is attached, the voltage across a solar cell is commonly referred to as  $V_{pv}$ . The micro grid converter's insulated gate bipolar transistor (IGBT) switches are designated as  $S_1$ ,  $S_2$ ,  $S_3$ , and  $S_4$ . The user's input field is blank. In a quadratic boost converter, the letter  $S$  represents the switch. The user's input field is blank. The symbols  $R_{Ldc}$  and  $R_{Lac}$  are used to represent DC and AC linear loads, respectively. The user's input field is blank.

These equations are commonly used to represent the nonlinear load's connected resistor and inductor to the single bridge rectifier. Their official names are  $L_{nl}$  and  $R_{nl}$ . The part of the bidirectional converter for super capacitors that is directly connected to the inductor is called the Low-Side Converter, or LSC for short. The super capacitor bidirectional converter's integrated gate bipolar transistor (IGBT) switches are referred to as  $SS_1$  and  $SS_2$ , respectively. Last but not least,  $L_b$  is the usual name for the connected resistor and inductor to  $L_{nl}$ . An output voltage of the DC-DC converter must meet the necessary threshold for low-voltage solar systems to provide the DC-link voltage that is required. The user's input field is blank. Photovoltaic (PV) systems use quadratic boost converters to achieve a high conversion ratio and ensure great performance throughout a broad voltage range [7]. The user's input field is blank. A bidirectional boost DC-DC converter (BDDC) handles the regulation of power flow from the power grid to energy storage devices like batteries and supercapacitors. The user's input field is blank. By connecting to the main power supply, the device may control the flow of energy via a Voltage Supply Converter (VSC).

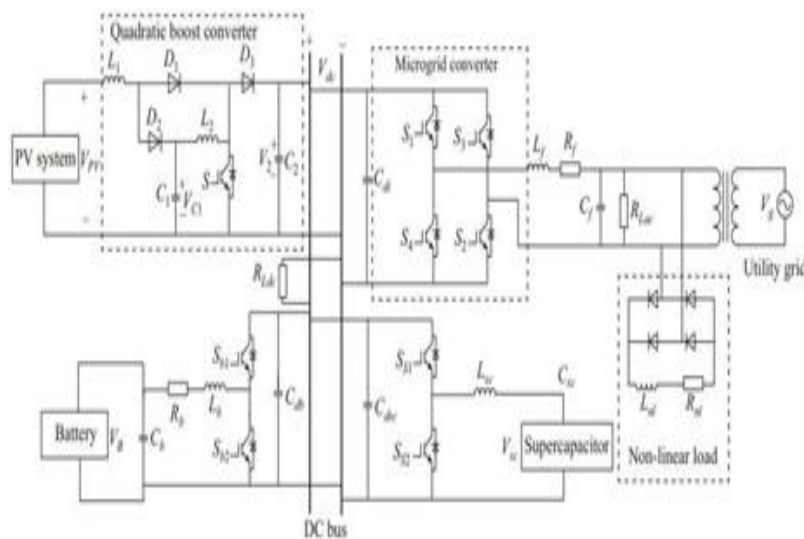
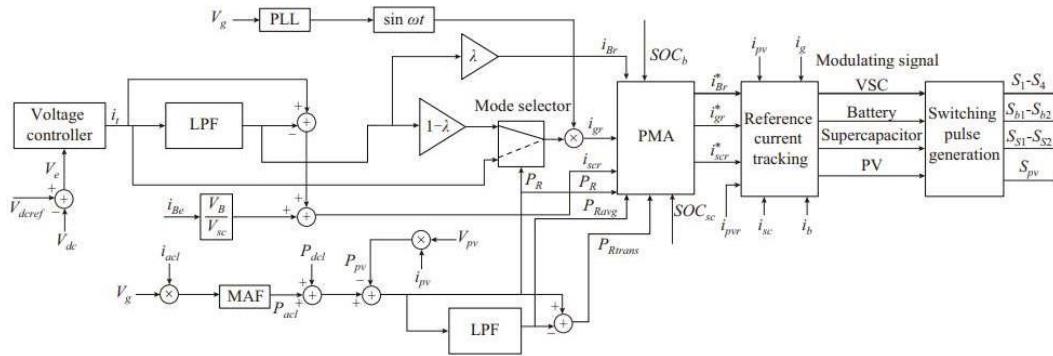


Fig. 1 Architecture of grid-coupled PV with HESS



**Fig. 2 Suggested power management arrangement for grid-connected system**

**III. REFERENCE CURRENT GENERATION FOR GRID AND HESS**

The operational dynamics of a grid-coupled DC microgrid are determined by the means of charging it, which may include energy storage devices, solar (PV) systems, and the utility grid. Ensuring a complete balance of power is crucial for establishing and maintaining stability in any system. When there is a balance of all forces, we say that we are in equilibrium:

$$P_g(t) + P_{pv}(t) + P_B(t) + P_{sc}(t) - P_l(t) = P_t(t) \tag{1}$$

The total power consumption of DC and AC loads may be determined using the formula  $P_l(t)$

$= P_{dcl}(t) + P_{acl}(t)$ . So, grid power, green power, batteries, and supercapacitors are represented by  $P_g(t)$ ,  $P_B(t)$ , and  $P_{sc}(t)$ , respectively. As illustrated by  $V_{dc}$  [6], the power balance is maintained between power output and power consumption. The overall power required for DC-link power balancing consists of two components: the average power  $P_t(t)$  and the transient power  $P' t(t)$ . You can see the current and total power values in the table below:

$$P_i(t) = P_t(t) + P'_i(t) = V_{dc} i_i(t) \tag{2}$$

$$i_i(t) = \frac{\bar{P}_t(t)}{V_{dc}} + \frac{P'_i(t)}{V_{dc}} = \bar{i}_i(t) + i'_i(t) \tag{3}$$

Where

In this context, " $i(t)$ " refers to the operational current, " $\bar{i}(t)$ " to the average value, and " $i'(t)$ " to the temporary value. The DC bus operational current is generated by the voltage controller, as shown in (4).

$$i_i(t) = \bar{i}_i(t) + i'_i(t) = K_{pvd} V_e + K_{ivd} \int v_e dt \tag{4}$$

The figures  $V_e$ ,  $K_{pvd}$ , and  $K_{ivd}$  represent the voltage control loop's proportional, integral, and DC-link error voltages, respectively. The LPF [9] separates the current before sending it to the grid, batteries, and photovoltaic cells. A large quantity of electrical current is supplied by the supercapacitor.

$$\bar{i}_i(s) = \frac{\omega_c}{s + \omega_c} i_i(s) \tag{5}$$

$$\begin{cases} i_{Br}(s) = \lambda \bar{i}_i(s) \\ i_{gr}(s) = (1 - \lambda) \bar{i}_i(s) \end{cases} \tag{6}$$

$$i'_i(s) = \left( 1 - \frac{\omega_c}{s + \omega_c} \right) i_i(s) \tag{7}$$

Locate the grid reference current, battery reference current, power sharing coefficient, and LPF cut-off frequency. Their proper sequence is as follows. The lowest frequency that can be accommodated by the low-pass filter (LPF) is determined to be 6.283 radians per second. The primary function of the sharing coefficient is to maintain a constant state of charge (SOC) in the battery over an extended period of time by reducing the current change rate under typical operating conditions and anticipated power variations [9]. The sharing coefficient will have a different value when the battery is completely charged (SOCb). Table I [5] shows that the state of charge (SOC) has two upper and lower bounds, denoted as U and L, respectively. As an illustration of the insufficient power mode (IPM), this is provided.

TABLE I LOGIC FOR  $\lambda$  IN IPM

$SOC_b(t)$	$\lambda$	$1-\lambda$
$0.7 < SOC_b < U$	1.0	0
$0.5 < SOC_b < 0.7$	0.6	0.4
$0.1 < SOC_b < 0.5$	0.3	0.7
$SOC_b < L$	0	1.0

IV. PROPOSED METHOD FOR POWER MANAGEMENT

In order to determine the system's operating status, the PMA considers the power supply, which includes both generated and discharged power. Setting (8) provides the following definitions of the three power modes of operation (PR).

$$P_R = P_l - P_{pv} \tag{8}$$

- 1) IPM:  $PR > 0$ .
- 2) Sufficient power mode (SPM):  $PR < 0$ .
- 3) Floating power mode (FPM):  $PR = 0$ .

Every power mode has its own set of guidelines that are determined by the supercapacitor and battery's state of charge (SOC). A technique known as Coulomb counting may be employed to determine the State of Charges (SOC<sub>b</sub> and SOC<sub>sc</sub>) of batteries and supercapacitors. This method is illustrated in Figure.3 [9], [5]. Here we can see the theoretical capacity (i<sub>b</sub>), initial state of charge (SOC (b<sub>0</sub>), initial supercapacitor state of charge (SOC<sub>sc0</sub>), current (CN), and initial state of charge (SOC) (CN) of the battery and supercapacitor, respectively.

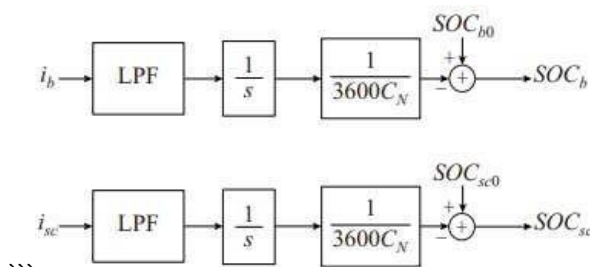


Fig.3 SOC calculation using Coulomb counting method

IPM When this mode of operation is used, it is discovered that the power needs exceed the energy

provided by the solar (PV) system. The supercapacitor effectively manages short-term power demand until it hits its lower state of charge (SOC) limit. The main grid, PV, and battery collaborate to manage average power loss until the battery's state of charge (SOC) falls below specified limits. If the supercapacitor's state of charge (SOC) goes below the lower level, power fluctuations are handled by the main grid. Table II shows the viability of several IPM designs dependent on the state of charge (SOC) of the battery and supercapacitor. The sign \* indicates the battery reference current in the power management programme. Table III contains the information required for power control in IPM. P<sub>loss</sub>, i<sub>loss</sub>, P<sub>R</sub>, and P<sub>R</sub> reflect the various characteristics of the system's power demand. It consists of the overall average power demand, the transient component, and general power losses.

TABLE II FUNCTIONAL DESIGNS IN

IPM

SOC limit	Reference current generation
$SOC_b > L$ and $SOC_{sc} > L$	$i_{Br}^* = \lambda \bar{i}_t$ , $i_{scr}^* = i_t'$ , $i_{gr}^* = (1-\lambda) \bar{i}_t$
$SOC_b < L$ and $SOC_{sc} > L$	$i_{Br}^* \cong 0$ , $i_{scr}^* = i_t'$ , $i_{gr}^* = \bar{i}_t$
$SOC_b > L$ and $SOC_{sc} < L$	$i_{Br}^* = \lambda \bar{i}_t$ , $i_{scr}^* \cong 0$ , $i_{gr}^* = (1-\lambda) \bar{i}_t + i_t'$
$SOC_b < L$ and $SOC_{sc} < L$	$i_{Br}^* \cong 0$ , $i_{scr}^* \cong 0$ , $i_{gr}^* = i_t$

**TABLE III**  
POWER MANAGEMENT IN IPM

SOC limit	Reference power
$SOC_b > L$ and $SOC_{sc} > L$	$P_B^*(t) = \lambda \bar{P}_R, P_{sc}^*(t) = P_R', P_g(t) = (1 - \lambda) \bar{P}_R + P_{loss}$
$SOC_b < L$ and $SOC_{sc} > L$	$P_B^*(t) \equiv 0, P_{sc}^*(t) = P_R', P_g(t) = \bar{P}_R + P_{loss}$
$SOC_b > L$ and $SOC_{sc} < L$	$P_B^*(t) = \lambda \bar{P}_R, P_{sc}^*(t) \equiv 0, P_g(t) = (1 - \lambda) \bar{P}_R + P_R' + P_{loss}$
$SOC_b < L$ and $SOC_{sc} < L$	$P_B^*(t) \equiv 0, P_{sc}^*(t) \equiv 0, P_g(t) = \bar{P}_R + P_{loss}$

### SPM

The photovoltaic system generates excess electricity when this mode of operation is employed. The battery and supercapacitor are recharged using the excess power until they achieve their desired state of charge (SOC). When batteries and supercapacitors are fully charged or overcharged, the excess power is sent to the main grid using a voltage source converter (VSC). The applications of SPM are detailed in Table IV, and its power handling capabilities are discussed in further depth in Table V.

TABLE IV FUNCTIONAL DESIGNS IN

### SPM

SOC limit	Reference current generation
$SOC_b < U$ and $SOC_{sc} < U$	$i_{Br}^* = i_{B, ch}, i_{scr}^* = i_{sc, ch}, i_{gr}^* = i_t$
$SOC_b < U$ and $SOC_{sc} > U$	$i_{Br}^* = i_{B, ch}, i_{scr}^* = i_t', i_{gr}^* = i_t - i_{scr}$
$SOC_b > U$ and $SOC_{sc} < U$	$i_{Br}^* \equiv 0, i_{scr}^* = i_{sc, ch}, i_{gr}^* = i_t$
$SOC_b > U$ and $SOC_{sc} > U$	$i_{Br}^* \equiv 0, i_{scr}^* = i_t', i_{gr}^* = i_t - i_{scr}$

**TABLE V**  
POWER MANAGEMENT IN SPM

SOC limit	Reference power
$SOC_b < U$ and $SOC_{sc} < U$	$P_B^*(t) = -P_{Br}, P_{sc}^*(t) = -P_{scr}, P_g(t) = P_{loss}$
$SOC_b < U$ and $SOC_{sc} > U$	$P_B^*(t) = -P_{Br}, P_{sc}^*(t) \equiv 0, P_g(t) = P_{loss}$
$SOC_b > U$ and $SOC_{sc} < U$	$P_B^*(t) \equiv 0, P_{sc}^*(t) = -P_{scr}, P_g(t) = P_{loss}$
$SOC_b > U$ and $SOC_{sc} > U$	$P_B^*(t) \equiv 0, P_{sc}^*(t) \equiv 0, P_g(t) = P_{loss} - P_R$

## V. CONTROL STRUCTURE FOR CONVERTERS MODELING OF CONVERTER CONTROL FOR HESS

Create a reference current  $i^*_{Br}$  as part of the converter control; use the integrated power module's state of charge (SOC) to determine the average power sharing constant; and run the powermanagement algorithm (PMA). Pulse width modulation, or PWM for short, is defined in Figure 4. Here are the specifications for the bidirectional converter that is connected to the battery: the modulating signal  $B$  and the reference current  $i^*_{Br}(t)$ :

$$i^*_{Br}(t) = f_{B, PMA} \lambda \frac{1}{T_B} \int_{t_0 - T_B}^{t_0} i_t(t) dt \quad (9)$$





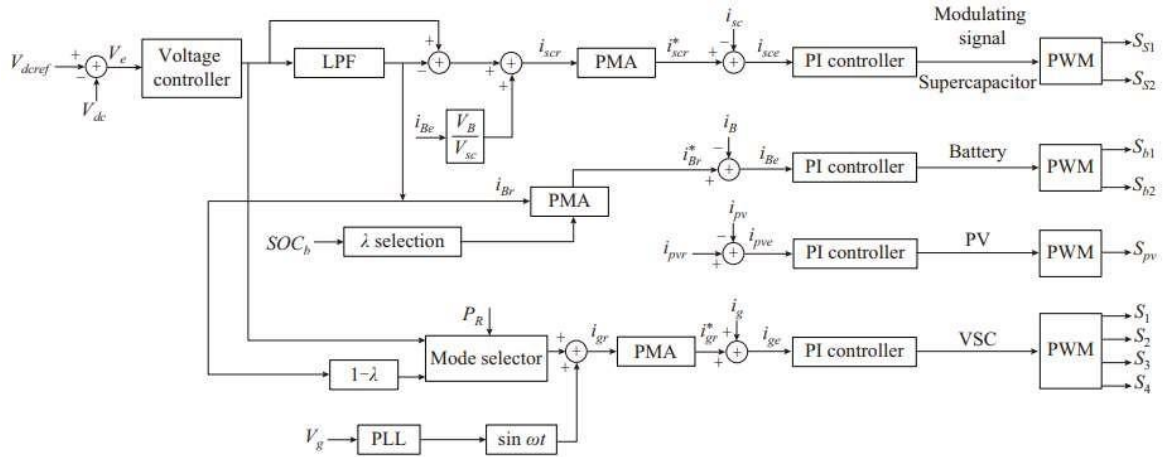


**Fig. 4 Converter control for super capacitor, battery, PV, and utility grid**

**MODELING OF CONTROL FOR PV CONVERTER**

If you want to be sure the system works in all three of the unusual circumstances mentioned in Section II, you can adjust the reference current of the PV converter. A comparison of the actual current flowing through the high gain PV converter with the selected PV reference current ( $i_{pvr}$ ) is illustrated in Figure 3.1. PI regulators ensure that this resemblance is controlled.

**VII. SIMULATION RESULTS AND DISCUSSION**

By running simulations in the MATLAB 9.6.1.1072779 (R2019a) environment, we can confirm that the proposed method works. A graphical programming interface called Simulink was developed to offer a modelling system that is easy for users to understand and utilise. It allows users to solve numerical issues using a graphical user interface rather than requiring computer code. Annotations to the backdrop, signals, and blocks make up a model. Mathematical functions are represented using blocks. Numbers of inputs and outputs change.

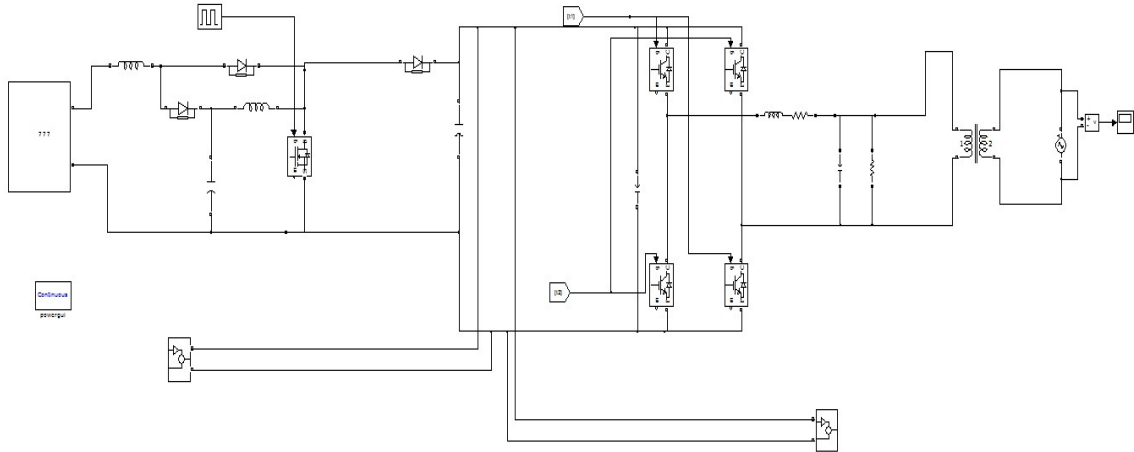


**Fig.5 simulation model**

**TABLE VI**

Parameters Used For System Simulation are listed below,

Specification	Parameter	Value
PV array	$V_{pv}$	40 V
	$I_{pv}$	20 A
Supercapacitor	$V_{sc}$	16.2 V
	$i_p$	200 A
	$C_{sc}$	58 F
	$i_{sc}$	19 A
Battery	$C_b$	14 Ah
	$V_B$	12 V
Battery BDDC	$R_b$	0.5 $\Omega$
	$L_b$	5 mH
	$C_b$	220 $\mu$ F
	$C_{db}$	220 $\mu$ F
Supercapacitor BDDC	$L_{sc}$	5 mH
	$C_{dsc}$	220 $\mu$ F
VSC	$L_f$	10 mH
	$C_f$	1 $\mu$ F
	$C_{df}$	2200 $\mu$ F
Quadratic boost PV converter	$L_1=L_2$	5 mH
	$C_1$	110 $\mu$ F
	$C_2$	220 $\mu$ F
Linear and non-linear load parameters	$R_{Ldc}$	50 $\Omega$
	$R_{Lac}$	10 $\Omega$
	$R_{nl}$	30 $\Omega$
	$L_{nl}$	1 mH
Utility grid	$V_g$	230 V
	$f$	50 Hz
DC bus voltage	$V_{dc}$	100 V
LPF	$f_{LPF}$	1 Hz
MAF	$f_{MAF}$	100 Hz

PERFORMANCE WITH VARIATION IN PV POWER

Figures 6 and 7 show how well the control mechanisms work when PV power varies. The system's power output changes at t= 2 seconds owing to a radiation drop from 1000 W/m2 to 600 W/m2. Figure 4.2 shows PV power production decreasing after two seconds. Figure 6 shows that theDC bus voltage returns to normal after 0.15 seconds. But this is 1 V below the intended value. According to IEEE standard 929-2000 [9], this drop is acceptable. This occurs regardless of solar power variation. Supercapacitors manage the switchover's transient power boost. Grid and battery devices work together to regulate DC voltage and average component. Using a battery and supercapacitor in solar PV generating decreases voltage loss during changeover and voltage stability.Less setup time means the DC-bus voltage enters the error range faster.

Fig. 6 Voltages of DC link, battery, and super capacitor with PV power variation

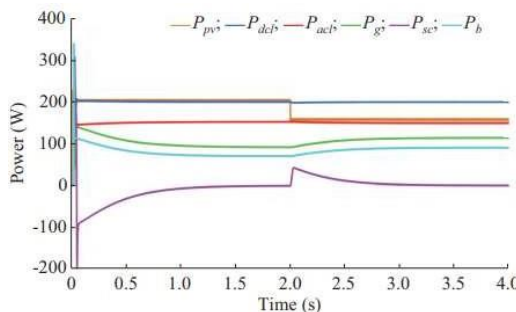
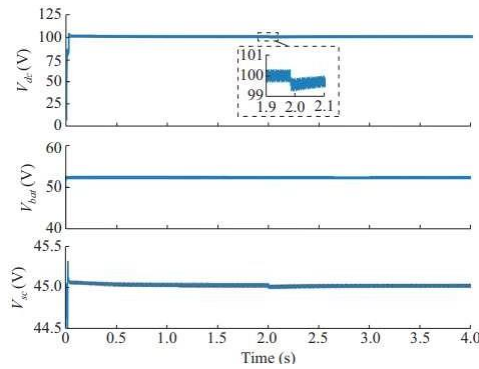


Fig. 7 Power of PV, DC load, AC load, utility grid, super capacitor, and battery with PV powervariation  
Grid current THD fluctuates with PV output.





PERFORMANCE WITH VARIATION IN LOAD

The effectiveness of the control methods in the presence of fluctuating loads and insufficient power is seen in Figures 4.4 and 4.5. With RLdc= 50 and RLdc= 25 at t = 2 seconds, the DC load increases as the linear DC load decreases. Figure 4.4 displays a rapid shift in the DC input power at time t = 2 seconds. The DC bus voltage is stabilised by the power grid's average management, while the batteries and short-term power are managed by the supercapacitor. Accordingly, a 2 V reduction in DC bus voltage is well within the permissible limit [8]. It reverts to its initial state in 0.2 seconds, regardless of how rapidly the load requirements vary.

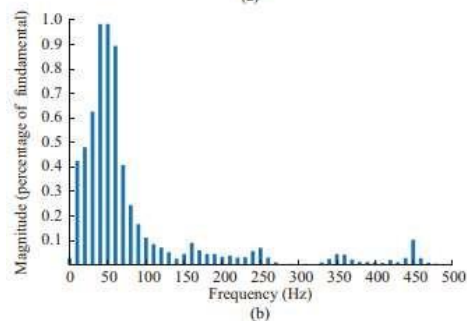
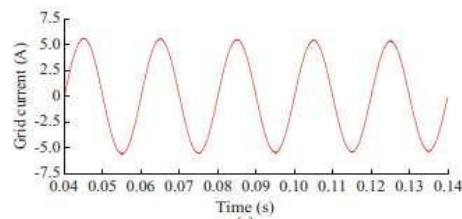


Fig .8 THD of utility grid current with PV power variation

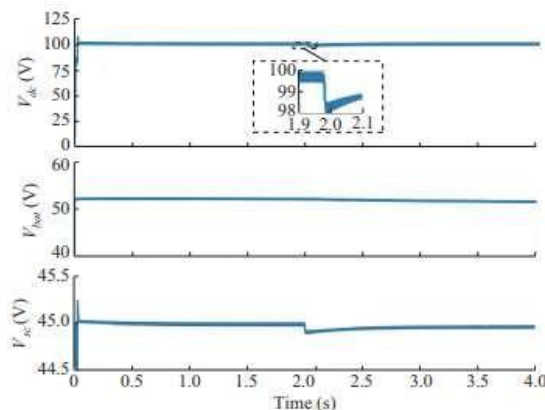


Fig. 9 Voltages of DC link, battery, and super capacitor under load variation

When the load fluctuates, the frequency waveform is shown in Figure 4.6. A frequency variation of 0.01 Hz occurs due to a sudden increase in the load at time t = 2 s.

### VIII. CONCLUSION

Hybrid energy storage devices that integrate with grid-connected solar systems provide a novel approach to power management. To ensure precise power quality features, HESSs must be employed with bidirectional power flow. The aims of the proposed method—which include controlling DC voltage more quickly, regulating voltage and frequency, managing power quality, and maintaining a storage system state of charge (SOC) within acceptable limits—are supported by the simulation findings. In order to evaluate the efficacy of the control approach under consideration, we may compare it to comparable systems using power quality metrics as settling time, overshoot/undershoot, and total harmonic distortion (THD). The proposed layout does not account for demand at either peak or off-peak times. To enhance power management, these data might be included. The results of grid-connected application simulations support the proposed approach. Therefore, it is compatible with autonomous microgrid systems. Then, to guarantee the system's stability, signal analysis might be performed.

### IX. REFERENCES

- [1] S. K. Kollimalla and M. K. Mishra, "A novel adaptive P&O MPPT algorithm considering sudden changes in the irradiance," *IEEE Transactions on Energy Conversion*, vol. 29, no. 3, pp. 602-610, May 2014.
- [2] S. Mishra and R. K. Sharma, "Dynamic power management of PV based islanded micro grid using hybrid energy storage," in *Proceedings of IEEE 6th International Conference on Power Systems (ICPS)*, New Delhi, India, Mar. 2016, pp. 1-6.
- [3] C. Natesan, S. Ajithan, S. Chozhavendhan et al., "Power management strategies in micro grid: a survey," *International Journal of Renewable Energy Research*, vol. 5, no. 2, pp. 334-340, Jan. 2015.
- [4] Z. Yi, W. Dong, and A. H. Etemadi, "A unified control and power management scheme for PV-battery-based hybrid micro grids for both grid-connected and islanded modes," *IEEE Transactions on Smart Grid*, vol. 9, no. 6, pp. 5975-5985, Nov. 2018.
- [5] S. Pannala, N. Patari, A. K. Srivastava et al., "Effective control and management scheme for isolated and grid connected DC micro grid," *IEEE Transactions on Industry Applications*, vol. 56, no. 6, pp. 1-14, Dec. 2020.
- [6] P. Singh and J. S. Lather, "Variable structure control for dynamic power-sharing and voltage regulation of DC micro grid with a hybrid energy storage system," *International Transaction Electrical Energy System*, vol. 30, no. 9, pp. 1-20, Jun. 2020.
- [7] N. R. Tummuru, U. Manandhar, A. Ukil et al., "Control strategy for AC-DC micro grid with hybrid energy storage under different operating modes," *Electrical Power and Energy Systems*, vol. 104, pp. 807- 816, Jan. 2019.
- [8] J. Hu, Y. Shan, Y. Xu et al., "A coordinated control of hybrid AC/DC micro grids with PV-wind-battery under variable generation and load conditions," *Electrical Power and Energy Systems*, vol. 104, pp. 583- 592, Jan. 2019.
- [9] H. Mahmood, D. Michaelson, and J. Jiang, "A power management strategy for PV/battery hybridsystems in islanded micro grids," *IEEE Journal of Emerging and Selected Topics in Power Electronics*, vol. 2, no. 4, pp. 870-882, Jun. 2014.
- [10] P. Sanjeev, N. P. Padhy, and P. Agarwal, "Peak energy management using renewable integrated DC micro grid," *IEEE Transactions on Smart Grid*, vol. 9, no. 5, pp. 4906-4917, Sept.

#### Author(s) Profile:



**Mr. A V V Vishnu** from Andhra Pradesh as completed his graduation in Annamacharya Institute of Technology & Sciences, Tirupati in the stream of Electrical & Electronics Engineering in 2022. Presently he is pursuing his master degree in Power Electronics and Electrical Drives from VEMU institute of Technology, P.Kothakota, Chittoor district, Andhra Pradesh, India.



**Mr. M. Murali** from Andhra Pradesh as completed his Master degree from Srinivasa Institute of Technology & Management Studies, Chittoor in 2009. Presently he is working as Associate Professor in the department of Electrical & Electronics Engineering, VEMU institute of Technology, P.Kothakota, Chittoor district, Andhra Pradesh, India.



**Dr. A. Hema Sekhar** from Andhra Pradesh as completed his Doctor of Philosophy in SV University, Tirupati in the stream of Electrical & Electronics Engineering in 2016. Presently he is working as Professor & HOD in the department of Electrical & Electronics Engineering, VEMU institute of Technology, P.Kothakota, Chittoor district, Andhra Pradesh, India.



**Mr. P. I. D. T. Baladuraikannan** from Tamil Nadu as completed his Master degree from Mailam Engineering College, Tindivanam in 2011. Presently he is working as Associate Professor in the department of Electrical & Electronics Engineering, VEMU institute of Technology, P.Kothakota, Chittoor district, Andhra Pradesh, India.